RISK HEMOLYSES REGIONS DETECTION IN A VENTRICULAR ASSIST DEVICE BY COMPUTATIONAL FLUID DYNAMICS

Guilherme B Lopes Jr., Federal University of Triangulo Mineiro, e-mail (lopesjr.gb@gmail.com)
Luben Cabezas-Gómez, São Carlos School of Engineering, University of São Paulo, e-mail (lubencg@sc.usp.br)
Eduardo G. P. Bock, Federal Institute of São Paulo, e-mail (eduardobock@gmail.com)

Abstract. *This paper presents a methodology for analyzing risk hemolysis regions detection in ventricular assist devices. It is based on detecting flow regions with high stresses values. The flow stresses are calculated using the numerical results obtained with computational fluid dynamics techniques. In order to consider the flow turbulence four two-equation models are used. The obtained results are useful, and show the potential of the developed procedure.*

Key-words*: VAD simulations, Turbulence, Hemolysis, Critical stresses.*

1. INTRODUCTION

Several advances in biomedical engineering have reached significant improvements in Ventricular Assist Devices (VAD) project development. Supporting this development, Computational Fluid Dynamics (CFD) has been applied to reach detailed analyses based on simulated scenarios.

In the present work, risk hemolysis regions detection is purposed based on critical stress calculated by CFD in a VAD. The critical stress determination is based on literature and the formulation for stress approximation in the CFD simulations is presented. The blood flow is also analyzed with two different turbulence models.

2. NUMERICAL METHODOLOGY

In this section is described the numerical methodology followed. For more detailed information, it is encouraged to read Lopes Jr (2016) and Lopes Jr. et al. (2016a,b).

2.1. Geometry and Mesh

The geometry (Fig. 1) studied in this work is based on Bock et al. (2011). In their work, a VAD is purposed in experimental tests. Here the geometry is used for simulating the scenarios purposed in section 2.2.

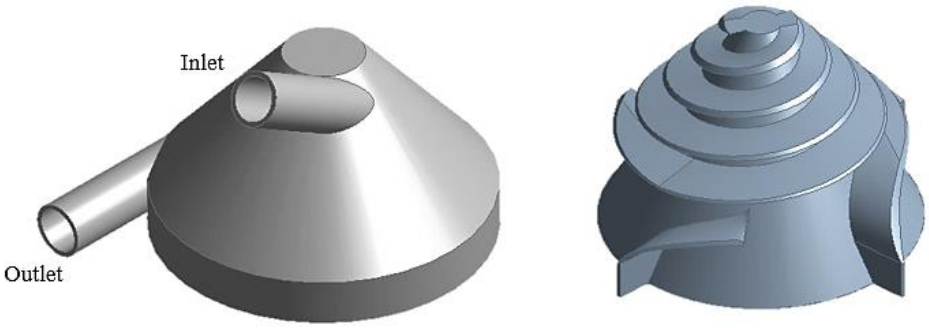

Figure 1: geometry studied, based on Bock et al. (2011) and detailed on Lopes Jr. (2016).

The mesh, representing the fluid domain discretized, is on Fig. 2. It contains two different regions: inertial and non-inertial domains, because the multiple reference frame methodology was applied. In the inertial domain, it was applied around 220 elements/mm³, while in the non-inertial (around the rotor), there are 330 elements/mm³.

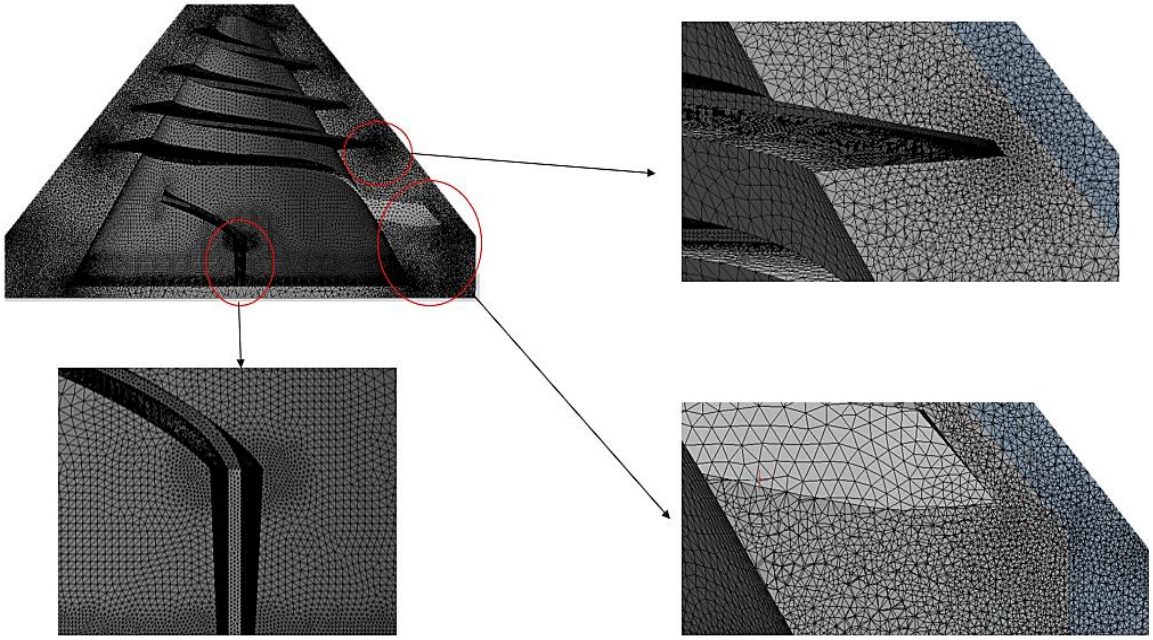

Figure 2: mesh details from an orthogonal view from rotor axe, from Lopes Jr. (2016)

2.2. General Fluid Flow Modelling and Scenarios Applied

The fluid flow was simulated using Navier-Stokes equations for Newtonian fluids. The stresses inside the blood pump are high, so the blood here was treated as Newtonian (MERRIL, 1969). The boundary layer thickness is supposed to be thin enough to ignore their effects on the mean flow, dominated by turbulence and advective influence.

Turbulence was considered. Reynolds-Avarage Navier-Stokes (RANS) two-equation models were applied. According to literature (FRAZER et al., 2012; SONG et al., 2010, for example), two models applications are studied here: standard $\kappa - \varepsilon$, RNG $\kappa - \varepsilon$, standard $\kappa - \omega$, and SST $\kappa - \omega$.

In order to solve the problem, the coupled pressure-velocity relation was solved by SIMPLEC method, using second order up-wind schemes. Multiple reference frames were applied, so steady-state was considered. Implicit steady-state method was applied for better convergence as well.

Loop test scenario was applied as condition. For the VAD presented, it represents 2000 rpm rotor speed and 95,51 mmHg pressure increase.

2.3. Stress Estimation

For stress calculation inside the flow region, it was considered the stress tensor for turbulent flows. Equation (1) is presented for this purpose:

$$\overline{\boldsymbol{\tau}}_{ji} = (\mu + \mu_t)\left(\frac{\partial \overline{V}_i}{\partial x_j} + \frac{\partial \overline{V}_j}{\partial x_i}\right) - \frac{2}{3}\rho k \delta_{ij} \tag{1}$$

Thus:

$$\overline{\boldsymbol{\tau}}_{ji} = 2(\mu + \mu_t)S_{ij} - \frac{2}{3}\rho k \delta_{ij} \tag{2}$$

The magnitude of the tensor can be expressed as:

$$\|\overline{\boldsymbol{\tau}}\| = \sqrt{\overline{\boldsymbol{\tau}} : \overline{\boldsymbol{\tau}}} = \sqrt{\overline{\boldsymbol{\tau}}_{ji}\overline{\boldsymbol{\tau}}_{ji}} \tag{3}$$

By the relation stress-strain:

$$\overline{\boldsymbol{\tau}}_{ji}\overline{\boldsymbol{\tau}}_{ji} = \left(2(\mu+\mu_t)S_{xx} - \frac{2}{3}\rho k\right)^2 + \left(2(\mu+\mu_t)S_{xy}\right)^2 + (2(\mu+\mu_t)S_{xz})^2 + \left(2(\mu+\mu_t)S_{yy} - \frac{2}{3}\rho k\right)^2 + \left(2(\mu+\mu_t)S_{yx}\right)^2 + \left(2(\mu+\mu_t)S_{yz}\right)^2 + \left(2(\mu+\mu_t)S_{zz} - \frac{2}{3}\rho k\right)^2 + \left(2(\mu+\mu_t)S_{zy}\right)^2 + (2(\mu+\mu_t)S_{zx})^2 \quad (4)$$

Applying some algebra, it is possible to develop Eq. (4) to Eq. (8):

$$\overline{\boldsymbol{\tau}}_{ji}\overline{\boldsymbol{\tau}}_{ji} = \left(2(\mu+\mu_t)S_{xx} - \frac{2}{3}\rho k\right)^2 + \left(2(\mu+\mu_t)S_{xy}\right)^2 + (2(\mu+\mu_t)S_{xz})^2 + \left(2(\mu+\mu_t)S_{yy} - \frac{2}{3}\rho k\right)^2 + \left(2(\mu+\mu_t)S_{yx}\right)^2 + \left(2(\mu+\mu_t)S_{yz}\right)^2 + \left(2(\mu+\mu_t)S_{zz} - \frac{2}{3}\rho k\right)^2 + \left(2(\mu+\mu_t)S_{zy}\right)^2 + (2(\mu+\mu_t)S_{zx})^2 \quad (5)$$

$$\Rightarrow \overline{\boldsymbol{\tau}}_{ji}\overline{\boldsymbol{\tau}}_{ji} = \left(2(\mu+\mu_t)S_{xx} - \frac{2}{3}\rho k\right)^2 + \left(2(\mu+\mu_t)S_{yy} - \frac{2}{3}\rho k\right)^2 + \left(2(\mu+\mu_t)S_{zz} - \frac{2}{3}\rho k\right)^2 + 4(\mu+\mu_t)^2\left[(S_{xz})^2 + \left(S_{zy}\right)^2 + (S_{zx})^2 + \left(S_{yx}\right)^2 + \left(S_{yz}\right)^2 + \left(S_{xy}\right)^2\right] \quad (6)$$

$$\Rightarrow \overline{\boldsymbol{\tau}}_{ji}\overline{\boldsymbol{\tau}}_{ji} = \left(\frac{2}{3}\rho k\right)^2 - \frac{4}{3}(\mu+\mu_t)S_{xx}\rho k + \left(\frac{2}{3}\rho k\right)^2 - \frac{4}{3}(\mu+\mu_t)S_{yy}\rho k + \left(\frac{2}{3}\rho k\right)^2 - \frac{4}{3}(\mu+\mu_t)S_{zz}\rho k + 4(\mu+\mu_t)^2\left[(S_{xx})^2 + \left(S_{yy}\right)^2 + (S_{zz})^2 + (S_{xz})^2 + \left(S_{zy}\right)^2 + (S_{zx})^2 + \left(S_{yx}\right)^2 + \left(S_{yz}\right)^2 + \left(S_{xy}\right)^2\right] \quad (7)$$

$$\Rightarrow \overline{\boldsymbol{\tau}}_{ji}\overline{\boldsymbol{\tau}}_{ji} = 3\left(\frac{2}{3}\rho k\right)^2 - \frac{4}{3}(\mu+\mu_t)\rho k\left(S_{xx}+S_{yy}+S_{zz}\right) + 4(\mu+\mu_t)^2\left[(S_{xx})^2 + \left(S_{yy}\right)^2 + (S_{zz})^2 + (S_{xz})^2 + \left(S_{zy}\right)^2 + (S_{zx})^2 + \left(S_{yx}\right)^2 + \left(S_{yz}\right)^2 + \left(S_{xy}\right)^2\right] \quad (8)$$

For an incompressible fluid: $S_{xx} + S_{yy} + S_{zz} = \nabla.\vec{\overline{V}} = 0$; thus:

$$\Rightarrow \overline{\boldsymbol{\tau}}_{ji}\overline{\boldsymbol{\tau}}_{ji} = 3\left(\frac{2}{3}\rho k\right)^2 + 4(\mu+\mu_t)^2\left[(S_{xx})^2 + \left(S_{yy}\right)^2 + (S_{zz})^2 + (S_{xz})^2 + \left(S_{zy}\right)^2 + (S_{zx})^2 + \left(S_{yx}\right)^2 + \left(S_{yz}\right)^2 + \left(S_{xy}\right)^2\right] \quad (9)$$

The last term is the quadratic of strain magnitude tensor, so:

$$\Rightarrow \overline{\boldsymbol{\tau}}_{ji}\overline{\boldsymbol{\tau}}_{ji} = 3\left(\frac{2}{3}\rho k\right)^2 + 4(\mu+\mu_t)^2S^2 \quad (10)$$

$$\|\overline{\boldsymbol{\tau}}\| = \sqrt{\overline{\boldsymbol{\tau}}_{ji}\overline{\boldsymbol{\tau}}_{ji}} = \sqrt{3\left(\frac{2}{3}\rho k\right)^2 + 4(\mu+\mu_t)^2S^2} \quad (11)$$

If $S \gg \kappa$ or $\kappa \gg S$, both terms are similar to each other, so it could be resumed to Eq. 12, while kinetic turbulent energy and high strain rates are not coincident at the same cell, considering the effect on mean velocity and oscillatory velocity partially independent.

$$\|\overline{\boldsymbol{\tau}}\| \approx \frac{2}{3}\rho k\sqrt{3} + 2(\mu+\mu_t)S \quad (12)$$

If both might be considered, an error term might be considered or estimated by the order of error $\propto \sqrt{\frac{4}{3}\sqrt{3}\rho k(\mu+\mu_t)S}$.

The stress magnitude was compared to literature limits for hemolysis. So stresses above 450 Pa were considered critical.

3. RESULTS, DISCUSSIONS AND CONTRIBUTION

General results are presented in Fig. 3.

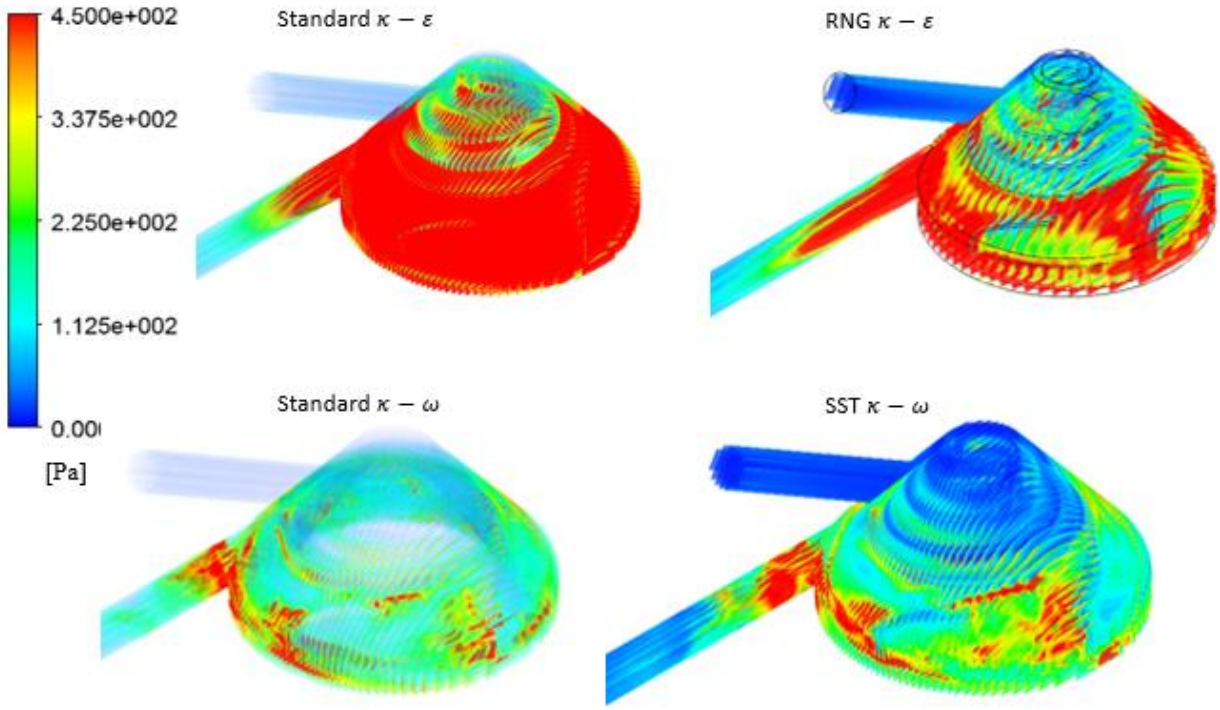

Figure 3: Hemolytic critical regions for each model tested

For each model, different regions are presented. Some similarities, although, are observed in the exit from the rotor to the outlet region. In $\kappa-\varepsilon$ based models for turbulence, the stresses in mean flow reach the critical stress in more sparced regions, while in $\kappa-\omega$ based models, they are concentrated in the high recirculation and turbulent expected regions, after the blades, for example. In the common region, at the rotor outlet, this behavior is due to the rapid loss of acceleration that increases the strain rates.

The results for critical stress regions are coherent to the physical problem and indicate improvement-need regions for the prototype. For both turbulence model simulations, estimating of these stresses could be possible and the results are similar, besides their differences in solving the closure problem.

4. CONCLUSIONS

The employed methodology for critical regions detection is useful and could found regions for improvement in VAD design. The differences from each turbulence model are sensitive and related to the critical stress specified.

A conclusive stress level is not definitive. Besides, any stress limit could be applied to this methodology. The stress estimation here presented is also relevant, but reliability analyses were not completely applied.

The $\kappa-\omega$ based models are more representative for the problem here purposed, when analyzed the physical expectation for the critical regions related to turbulence. But RNG $\kappa-\varepsilon$ is also representative with high stress magnitude values.

Turbulence stress measurement is a difficult task, even in numerical approaches. The presented equation for stress estimation can reduce uncertain and time simulation, since it allows RANS models to be applied.

The error magnitude in applying this equation might be investigated. On the other hand, when estimating stress magnitude in RANS model simulations, important turbulent effects on the stress are neglected. Equation 12 might reduce these simplifications.

Direct Numerical Simulations (DNS) are always encouraged. But complex events like the presented here are not possible yet, what reinforce the need of reach approximated models to improve the analyses and their accurate.

5. REFERENCES

BOCK, E., ANTUNES, P., LEAO, T., UEBELHART, B., FONSECA, J., LEME, J., UTIYAMA, B., da SILVA, C., CAVALHEIRO, A., SANTOS FILHO, D., DINKHUYSEN, J., BISCEGLI, J., ANDRADE, A., ARRUDA, C.. **Implantable Centrifugal Blood Pump with Dual Impeller and Double Pivot Bearing System: Electromechanical Actuator, Prototyping, and Anatomical Studies**. Artificial Organs, v.35, n.5, pg. 437-442, 2011.

FRASER, K.H., ZHANG, T., TASKIN, M.E., GRIFFITH, B.P., WU, J.Z.. **A Quantitative Comparison of Mechanical Blood Damage Parameters in Rotary Ventricular Assist Devices: Shear Stress, Exposure Time and Hemolysis Index**. Journal of Biomechanical Engineering, v.134, p. 081002-1- 081002-11, 2012.

LOPES JR., G.B.. **Metodologia para Análise Computacional de Escoamento Sanguíneo em Dispositivos de Assistência Ventricular**. PhD Thesis, presented in Mechanical Engineering Department of São Carlos Faculty of Engineering of São Paulo University, 2016.

LOPES JR, G B; GOMEZ, L. C. ; BOCK, E. G. P. . **Numerical Analyses for Low Reynolds Flow in a Ventricular Assist Device**. Artificial Organs, v. ., p. ., 2016.

LOPES JR, G B; GOMEZ, L. C. ; BOCK, E. G. P. **. Mesh Independency Analyses and Grid Density Estimation for Ventricular Assist Devices in Multiple Reference Frames Simulations**. TECHNISCHE MECHANIK, v. 36, p. 190-198, 2016.

MERRILL, E.W.. **Rheology of Blood**. Physiological Reviews, v.49, n.4, 1969.

SONG, X., WOOD, H.G., DAY, S.W., OLSEN, D.B.. **Studies of Turbulence Models in a Computational Fluid Dynamics Model of a Blood Pump**. Artificial Organs, v.27, n10, p. 935-937, 2003.

6. ACKNOWLEGMENTS

The authors are grateful to our institutions: UFTM, IFSP and USP. Acknowledgments are also intended to FAPESP and CNPq.

7. INFORMATIONS RESPONSABILITY

The authors are fully responsible for the information provided in this paper.